

See discussions, stats, and author profiles for this publication at: <https://www.researchgate.net/publication/43158995>

# Mechanistic and Energetic Aspects of the Thermal and Photochemical Redox Chemistry of the Octanuclear Cubane Complexes, $\text{Fe III}_8 (\mu_4 -\text{O}_4)(\mu\text{-pyrazolate})_{12} \text{X}_4$ ( $\text{X} = \text{Cl}$ or $\text{Br}$ )

ARTICLE in THE JOURNAL OF PHYSICAL CHEMISTRY A · MAY 2010

Impact Factor: 2.69 · DOI: 10.1021/jp911644e · Source: PubMed

CITATIONS

2

READS

27

## 6 AUTHORS, INCLUDING:



G. Ferraudi

University of Notre Dame

187 PUBLICATIONS 2,617 CITATIONS

SEE PROFILE



Indranil Chakraborty

University of California, Santa Cruz

39 PUBLICATIONS 457 CITATIONS

SEE PROFILE



Raphael G Raptis

Florida International University

142 PUBLICATIONS 2,492 CITATIONS

SEE PROFILE



Aleaander Graham Lappin

University of Notre Dame

93 PUBLICATIONS 1,530 CITATIONS

SEE PROFILE

# Mechanistic and Energetic Aspects of the Thermal and Photochemical Redox Chemistry of the Octanuclear Cubane Complexes, $\text{Fe}^{\text{III}}_8(\mu^4\text{-O}_4)(\mu\text{-pyrazolate})_{12}\text{X}_4$ ( $\text{X} = \text{Cl}$ or $\text{Br}$ )

Guillermo Ferraudi,<sup>\*,†</sup> Dalice Piñero,<sup>‡</sup> Indranil Chakraborty,<sup>‡</sup> Raphael G. Raptis,<sup>‡</sup> A. Graham Lappin,<sup>§</sup> and Nicholas Berlin<sup>§</sup>

Radiation Research Building, Department of Chemistry, University of Notre Dame, Notre Dame, Indiana 46556, Department of Chemistry and the Institute for Functional Nanomaterials, University of Puerto Rico, San Juan, PR 00931-3346, and Department of Chemistry and Biochemistry, University of Notre Dame, Indiana 46556

Received: December 8, 2009; Revised Manuscript Received: March 28, 2010

The mechanisms of the thermal and photochemical redox reactions of clusters  $[\text{Fe}^{\text{III}}_8(\mu^4\text{-O}_4)(\mu\text{-Pz})_{12}\text{X}_4]$  ( $\text{Pz} = \text{pyrazolate anion}$ ,  $\text{X} = \text{Cl}$  or  $\text{Br}$ ) were investigated in this work. Reactions of the complexes with  $\text{e}^-_{\text{sol}}$ ,  $\text{C}^*\text{H}_2\text{OH}$ , and several powerful reducing transition metal complexes were investigated using the pulse radiolysis technique. Reaction rates of the outer-sphere electron transfer reactions with transition metal complexes had to be rationalized by invoking the formation of a  $[\text{Fe}^{\text{III}}_7\text{Fe}^{\text{II}}(\mu^4\text{-O}_4)(\mu\text{-Pz})_{12}\text{X}_4]^-$  intermediate or excited state. A transient species observed in the reaction of the  $\text{e}^-_{\text{sol}}$  with the cubanes can be either an excited state or a reaction intermediate mediating the formation of the stable product,  $[\text{Fe}^{\text{III}}_7\text{Fe}^{\text{II}}(\mu^4\text{-O}_4)(\mu\text{-Pz})_{12}\text{X}_4]^-$ . Photoredox reactions, characteristic of the ligand  $\text{X}^-$  to  $\text{Fe}(\text{III})$  charge transfer excited states, were observed in the 350 nm steady state and 351 nm laser flash irradiations of the cubanes. Quantum yields are limited by the rapid recombination of the photofragments. The charge transfer spectroscopy of the products was rationalized on the basis of parameters derived from the thermal electron transfer reactions.

## Introduction

Polynuclear, cluster type, Fe complexes have commanded considerable attention because of their multiple roles in chemistry, from bioinorganic chemistry to materials chemistry.<sup>1–4</sup> Thermodynamic stability and chemical versatility are respectively required of these materials for commercial applications and for the manifestation of properties such as catalytic activity. An interesting structural concept to achieve both is to coat a reactive kernel with inert substances such as nature does with proteins where metal active centers are protected inside the organic part of the macromolecule. This strategy has been explored with clusters  $[\text{Fe}^{\text{III}}_8(\mu^4\text{-O}_4)(\mu\text{-Pz})_{12}\text{X}_4]$  ( $\text{Pz} = \text{pyrazolate anion}$ ,  $\text{X} = \text{Cl}$  or  $\text{Br}$ ) (I). They

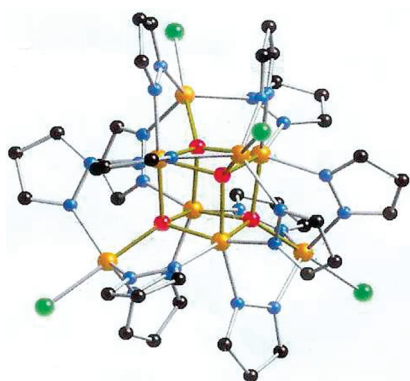
$[\text{Fe}^{\text{III}}_7\text{Fe}^{\text{II}}(\mu^4\text{-O}_4)(\mu\text{-Pz})_{12}\text{X}_4]^-$ , are produced when the first electron is added to the  $\text{Fe}_4\text{O}_4$  core of  $[\text{Fe}^{\text{III}}_8(\mu^4\text{-O}_4)(\mu\text{-Pz})_{12}\text{X}_4]$ . Other mixed-valence complexes produced by the sequential addition of up to four electrons are also stable in organic solvents.<sup>5</sup> The sturdiness of the  $\text{Fe}_4\text{O}_4$  cubane inside the protective Fe–pyrazolate shell is therefore demonstrated by the stability that the structure exhibits over these five oxidation states.<sup>5,6</sup>

The ability of  $[\text{Fe}^{\text{III}}_8(\mu^4\text{-O}_4)(\mu\text{-Pz})_{12}\text{X}_4]$  to behave as ground state and/or excited state oxidants is of a major relevance in applications of the  $[\text{Fe}^{\text{III}}_8(\mu^4\text{-O}_4)(\mu\text{-Pz})_{12}\text{X}_4]$  to the catalysis of redox reactions. The study of other well-known cubane oxidants has provided extensive information on the mechanistic details of intermolecular electron transfer processes.<sup>7–9</sup> However, concerning the  $[\text{Fe}^{\text{III}}_8]$ 's chemical and electrochemical reductions, little is known about these reactions and their mechanisms. The mechanism of the thermochemical and photochemical redox reactions of  $[\text{Fe}^{\text{III}}_8(\mu^4\text{-O}_4)(\mu\text{-Pz})_{12}\text{X}_4]$  are the focus of this work. Pulse radiolysis was applied to the study of the mechanism of the electron transfer reactions between electron donors and  $[\text{Fe}^{\text{III}}_8(\mu^4\text{-O}_4)(\mu\text{-Pz})_{12}\text{X}_4]$ . In addition, the photobehavior of the  $[\text{Fe}^{\text{III}}_8(\mu^4\text{-O}_4)(\mu\text{-Pz})_{12}\text{X}_4]$  ( $\text{X} = \text{Cl}$  or  $\text{Br}$ ) complexes was investigated and rationalized on the basis of the mechanistic information obtained from the electron transfer reactions.

## Experimental Section

**Materials.**  $[\text{Fe}^{\text{III}}_8(\mu^4\text{-O}_4)(\mu\text{-Pz})_{12}\text{X}_4]$  ( $\text{X} = \text{Cl}$  or  $\text{Br}$ ) complexes were available from previous works.<sup>5,6</sup> Reagent quality materials and solvents were purchased from Aldrich and used as received.

**Photochemical Procedures.** Absorbance changes,  $\Delta A$ , occurring in a time scale longer than 10 ns were investigated at room temperature with a flash photolysis apparatus described elsewhere.<sup>10</sup> In these experiments, 10 ns flashes of 351 nm light were generated with a Lambda Physik SLL-200 excimer laser. The energy of the laser flash was attenuated to values equal to or less than 20 mJ/pulse by absorbing some of the laser light in



(I)  $[\text{Fe}^{\text{III}}_8(\mu^4\text{-O}_4)(\mu\text{-Pz})_{12}\text{X}_4]$

have a redox active cubane core,  $\text{Fe}_4\text{O}_4$ , inside a protective Fe–pyrazolate shell.<sup>5,6</sup> Stable mixed-valence complexes,

<sup>†</sup> Department of Chemistry, University of Notre Dame.

<sup>‡</sup> University of Puerto Rico.

<sup>§</sup> Department of Chemistry and Biochemistry, University of Notre Dame.

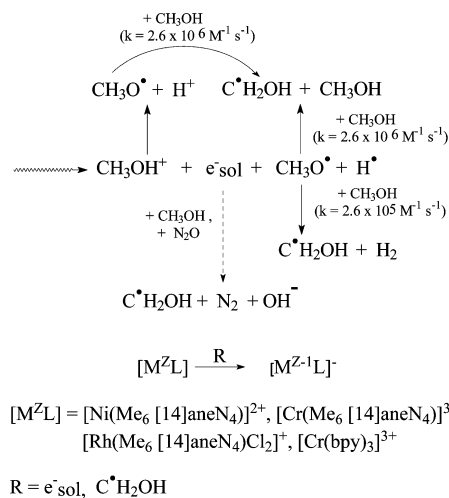
a filter solution of  $\text{Ni}(\text{ClO}_4)_2$  having the desired optical transmittance,  $T = I_t/I_0$  where  $I_0$  and  $I_t$  are respectively the intensities of the light arriving to and transmitted from the filter solution. The transmittance,  $T = 10^{-A}$ , was routinely calculated by using the spectrophotometrically measured absorbance,  $A$ , of the filter solution. A right angle configuration was used for the pump and the probe beams. Concentrations of the chromophores in the solution were adjusted to provide homogeneous concentrations of photogenerated intermediates over the optical path,  $l = 1$  cm, of the probe beam. To satisfy this optical condition, solutions were made with an absorbance equal to or less than 0.4 over the 0.2 cm optical path of the pump. These solutions were deaerated with streams of  $\text{N}_2$  before and during the photochemical experiments. Other conditions for these measurements are commented elsewhere in the Results.

Steady state irradiations were carried out with light from a 350 nm Rayonet lamp under optically dense conditions, i.e.,  $A > 2.5$  over 1 cm optical path at 350 nm. Light intensities,  $5 \times 10^{-4} > I_0 > 1 \times 10^{-4}$  Einstein  $\text{dm}^{-3} \text{min}^{-1}$ , were measured with Parker's actinometer.<sup>11</sup> Photolyses were irradiated in a reactor having two compartments formed by dual 1.0 and 0.2 cm optical path spectrophotometer cells. Solutions were irradiated in the 1.0 cm optical path cell and the spectrum of the solutions was recorded using either one or the other cell.

**Pulse-Radiolytic Procedures.** Pulse radiolysis experiments were carried out with a model TB-8/16-1S electron linear accelerator. The instrument and computerized data collection for time-resolved UV-vis spectroscopy and reaction kinetics have been described elsewhere in the literature.<sup>12</sup> Thiocyanate dosimetry was carried out at the beginning of each experimental session. The details of the dosimetry have been reported elsewhere.<sup>10</sup> The procedure is based on the concentration of  $(\text{SCN})_2^-$  radicals generated by the electron pulse in a  $\text{N}_2\text{O}$  saturated  $10^{-2}$  M  $\text{SCN}^-$  solution. In the procedure, the calculations were made with  $G = 6.13$  and an extinction coefficient,  $\epsilon = 7.58 \times 10^3 \text{ M}^{-1} \text{cm}^{-1}$  at 472 nm, for the  $(\text{SCN})_2^-$  radicals.<sup>12,13</sup> In general, the experiments were carried out with doses that in  $\text{N}_2$  saturated aqueous solutions resulted in  $(2.0 \pm 0.1) \times 10^{-6}$  to  $(6.0 \pm 0.3) \times 10^{-6}$  M concentrations of  $e^-_{\text{sol}}$ . In these experiments, solutions were prepared by the procedure indicated above for the photochemical experiments. The liquids were deaerated with streams of the  $\text{O}_2$ -free gas,  $\text{N}_2$ , or  $\text{N}_2\text{O}$ , which was required for the experiment. To radiolyze a fresh sample with each pulse, an appropriate flow of the solution through the reaction cell was maintained during the experiment. Other conditions used for the time-resolved spectroscopy of the reaction intermediates or in the investigation of the reaction kinetics are given in the Results. Radiolysis with ionizing radiation of  $\text{CH}_3\text{OH}$  has been reported elsewhere in the literature.<sup>14-16</sup> These studies have shown that pulse radiolysis can be used as a convenient source of  $e^-_{\text{sol}}$  and  $\text{C}^\bullet\text{H}_2\text{OH}$  radicals, Scheme 1.

The yield of  $e^-_{\text{sol}}$  in  $\text{CH}_3\text{OH}$  ( $G \sim 1.1$ ),<sup>14,15</sup> is about one-third of the  $G$ -value in the radiolysis of  $\text{H}_2\text{O}$  ( $G \sim 2.8$ ).<sup>14-16</sup> In solutions where  $e^-_{\text{sol}}$  was scavenged with  $\text{N}_2\text{O}$ , the  $\text{C}^\bullet\text{H}_2\text{OH}$  radical is the predominant product (yield >90%). Since  $e^-_{\text{sol}}$  and  $\text{C}^\bullet\text{H}_2\text{OH}$  have large reduction potentials, i.e.,  $-2.75$  V vs NHE for  $e^-_{\text{sol}}$  and  $-0.92$  V vs NHE for  $\text{C}^\bullet\text{H}_2\text{OH}$ , they have been used for the reduction of coordination complexes and for the study of electron transfer reactions. The Cr(III), Rh(III), and Ni(II) complexes in  $\text{N}_2$ -deaerated solutions trapped promptly the  $e^-_{\text{sol}}$  and  $\text{C}^\bullet\text{H}_2\text{OH}$  radicals,  $t_{1/2} \ll 10 \mu\text{s}$ , when used in concentrations  $\sim 5 \times 10^{-3}$  M, Scheme 1. In contrast, the reactions of  $e^-_{\text{sol}}$  and  $\text{C}^\bullet\text{H}_2\text{OH}$  radicals with  $\sim 10^{-4}$  M  $[\text{Fe}^{\text{III}}_8(\mu^4-$

## SCHEME 1



$\text{O}_4)(\mu\text{-Pz})_{12}\text{X}_4]$  ( $\text{X} = \text{Cl}$  or  $\text{Br}$ ) are much slower processes,  $t_{1/2} \gg 200 \mu\text{s}$ . The experimental conditions allow, therefore, the unimpeded study of the reactions between the reduction products and the Fe(III) complexes.

**Treatment of the Kinetic Data.** The reaction kinetics was investigated by following the absorbance change at given wavelengths of the spectrum and incorporating those changes in  $\xi = (\Delta A_{\text{inf}} - \Delta A_t)/(\Delta A_{\text{inf}} - \Delta A_0)$ .<sup>17</sup> In the expression of the dimensionless parameter  $\xi$ ,  $\Delta A_0$  is the absorbance change at the beginning of the reaction,  $\Delta A_t$  is determined at an instant  $t$  of the reaction and  $\Delta A_{\text{inf}}$  is determined at the end of the reaction. Values of  $\xi$  were fitted to the integrated rate law by a nonlinear least-squares method.

## Results

$[\text{Fe}^{\text{III}}_8(\mu^4\text{-O}_4)(\mu\text{-Pz})_{12}\text{X}_4]$  ( $\text{X} = \text{Cl}$  or  $\text{Br}$ ) behave as oxidants in the ground state electron transfer reactions communicated below. They also photodissociate in mixed-valence complexes and  $\text{X}^\bullet$  radicals when they are irradiated at wavelengths of the ligand to metal charge transfer, LMCT, transitions,  $\lambda_{\text{ex}} \sim 351$  nm. Using the Marcus theory of electron transfer reactions as a basis for the interpretation of the results, derived parameters from the thermal electron transfer reactions, such as the reorganization energies, have been used for a rationalization of the LMCT spectroscopy and photochemistry of the complexes.

**Electron Transfer Reactions of  $[\text{Fe}^{\text{III}}_8(\mu^4\text{-O}_4)(\mu\text{-Pz})_{12}\text{X}_4]$  ( $\text{X} = \text{Cl}$  or  $\text{Br}$ ) Complexes.** The pulse radiolysis technique was used for the generation and spectroscopic observation of the Fe(II) species formed when  $[\text{Fe}^{\text{III}}_8(\mu^4\text{-O}_4)(\mu\text{-Pz})_{12}\text{X}_4]$  complexes react with various radiolytically generated reductants. The reaction of  $e^-_{\text{sol}}$  with  $10^{-4}$  M  $[\text{Fe}^{\text{III}}_8(\mu^4\text{-O}_4)(\mu\text{-Pz})_{12}\text{X}_4]$  in  $\text{N}_2$ -deaerated MeOH is fast with a rate constant,  $k \sim 1.0 \times 10^{10} \text{ M}^{-1} \text{ s}^{-1}$ . In contrast to the reduction of  $[\text{Fe}^{\text{III}}_8(\mu^4\text{-O}_4)(\mu\text{-Pz})_{12}\text{X}_4]$  by  $e^-_{\text{sol}}$ , the Fe(III) complexes do not react with the radiolytically generated  $\text{C}^\bullet\text{H}_2\text{OH}$  radicals in solutions saturated with  $\text{N}_2\text{O}$ .

The spectra of the short-lived products produced when the cubanes are reduced by the  $e^-_{\text{sol}}$  are presented in Figures 1 and 2. When transient spectra were recorded with delays equal to or shorter than  $8 \mu\text{s}$  from the 1 ns radiation pulse, solvated electrons in the radiolyzed solution were identified by means of the characteristic absorption band at  $\lambda_{\text{max}} \sim 650$  nm.<sup>15,18</sup> The absorption band of the  $e^-_{\text{sol}}$  was not observed when transient spectra were recorded with delays longer than  $8 \mu\text{s}$  from the radiolysis pulse. Differences between the spectra recorded with delays longer than  $8 \mu\text{s}$  in either Figure 1 or Figure 2 have

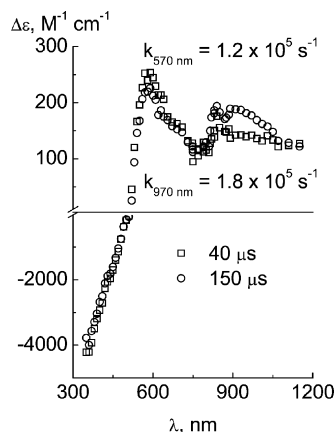


**Figure 1.** Transient spectra recorded at two different instants after  $e_{\text{sol}}^-$  reacted with  $10^{-4}$  M  $[\text{Fe}^{\text{III}}_8(\mu^4\text{-O}_4)(\mu\text{-Pz})_{12}\text{Cl}_4]$  in  $\text{N}_2$ -deaerated MeOH.  $\Delta\epsilon$  is the difference between the extinction coefficients of the products and the Fe(III) complex.

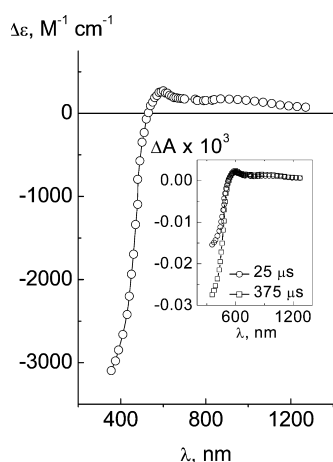
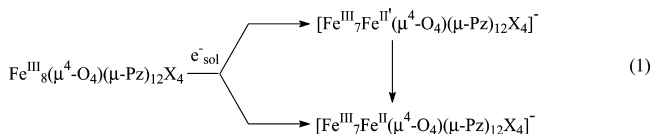


**Figure 2.** Difference spectrum of the transient product of the reaction of  $e_{\text{sol}}^-$  with  $10^{-4}$  M  $[\text{Fe}^{\text{III}}_8(\mu^4\text{-O}_4)(\mu\text{-Pz})_{12}\text{Br}_4]$  in  $\text{N}_2$ -deaerated MeOH. The inset shows transient spectra recorded during the formation of the products.

been associated with a process where an initially reduced complex, e.g.,  $[\text{Fe}^{\text{III}}_7\text{Fe}^{\text{II}}(\mu^4\text{-O}_4)(\mu\text{-Pz})_{12}\text{X}_4]^-$ , is converted to a more stable product, e.g.,  $[\text{Fe}^{\text{III}}_7\text{Fe}^{\text{II}}(\mu^4\text{-O}_4)(\mu\text{-Pz})_{12}\text{X}_4]^-$ , eq 1.



The changes in the spectrum between 350 and 1150 nm observed in a time scale longer than  $8 \mu\text{s}$  cannot be rationalized on the basis of Pz ligand reduction and they must be attributed to the formation of two different Fe(II) products. In agreement with this assignment, the bleach of the solution at wavelengths of the LMCT band, i.e.,  $\lambda_{\text{ob}} \leq 500$  nm in Figures 1 and 2, do not change during the transformation of the Fe(II) products shown in eq 1. Changes in the spectrum of the radiolyzed solution with time occur, however, at longer wavelengths, i.e.,  $\lambda_{\text{ob}} \geq 700$  nm, where the Fe(III)–Fe(II) intervalence band is located. The conversion of one product into the other is kinetically of first order in transient concentration and it was investigated by following the absorbance change at 570 nm and in the region of the intervalence band, i.e., at  $\lambda_{\text{ob}} = 970$  nm.

Similar rate constants  $k = 1.2 \times 10^5 \text{ s}^{-1}$  and  $k = 1.8 \times 10^5 \text{ s}^{-1}$  were calculated from absorbance changes occurring respectively at 570 and 970 nm.

The reductants  $\text{R}^-$ , listed in Table 1,<sup>19–27</sup> have less negative reduction potentials than the reduction potential of the  $e_{\text{sol}}^-$ ,  $E^0 \sim -2.75$  V vs. NHE. Pulse radiolysis was used for the generation of the  $\text{R}^-$  species in solutions where the concentrations of the parent Ni(II), Cr(III), and Rh(III) complexes prevented the reduction of  $[\text{Fe}^{\text{III}}_8(\mu^4\text{-O}_4)(\mu\text{-Pz})_{12}\text{X}_4]$  by  $e_{\text{sol}}^-$ . In contrast to the reaction of  $e_{\text{sol}}^-$  with  $[\text{Fe}^{\text{III}}_8(\mu^4\text{-O}_4)(\mu\text{-Pz})_{12}\text{X}_4]$  where  $[\text{Fe}^{\text{III}}_7\text{Fe}^{\text{II}}(\mu^4\text{-O}_4)(\mu\text{-Pz})_{12}\text{X}_4]^-$  was produced, only  $[\text{Fe}^{\text{III}}_7\text{Fe}^{\text{II}}(\mu^4\text{-O}_4)(\mu\text{-Pz})_{12}\text{X}_4]^-$  was observed in the reactions of  $\text{R}^-$  with  $[\text{Fe}^{\text{III}}_8(\mu^4\text{-O}_4)(\mu\text{-Pz})_{12}\text{X}_4]$ . Two reasons can be advanced for the different products of the reactions of  $e_{\text{sol}}^-$  and  $\text{R}^-$ . Because the reduction potentials of the reactants  $\text{R}^-$  are much more positive than the potential of  $e_{\text{sol}}^-$ , the driving forces for the formation of the  $[\text{Fe}^{\text{III}}_7\text{Fe}^{\text{II}}(\mu^4\text{-O}_4)(\mu\text{-Pz})_{12}\text{X}_4]^-$  product when  $\text{R}^-$  reacts with  $[\text{Fe}^{\text{III}}_8(\mu^4\text{-O}_4)(\mu\text{-Pz})_{12}\text{X}_4]$  are too small. Therefore, the formation of this product will be too slow by comparison to the formation of  $[\text{Fe}^{\text{III}}_7\text{Fe}^{\text{II}}(\mu^4\text{-O}_4)(\mu\text{-Pz})_{12}\text{X}_4]^-$ . Another reason is that  $[\text{Fe}^{\text{III}}_7\text{Fe}^{\text{II}}(\mu^4\text{-O}_4)(\mu\text{-Pz})_{12}\text{X}_4]^-$  could have escaped detection in the reactions of  $\text{R}^-$  with the Fe(III) complex. This is due to the limited experimental conditions that are available when  $\text{R}^-$  must be generated via the Scheme 1 while the reduction of the Fe(III) complexes by the  $e_{\text{sol}}^-$ , eq 1, must be avoided.

**Calculation of the  $[\text{Fe}^{\text{III}}_7\text{Fe}^{\text{II}}(\mu^4\text{-O}_4)(\mu\text{-Pz})_{12}\text{X}_4]^-$  Extinction Coefficients.** Extinction coefficients of the pulse radiolytically generated  $[\text{Fe}^{\text{III}}_7\text{Fe}^{\text{II}}(\mu^4\text{-O}_4)(\mu\text{-Pz})_{12}\text{X}_4]^-$  complexes were used in the calculation of the quantum yields of flash photolysis products. These photochemical experiments are described in the next section. The differences  $\epsilon_{\text{P}} - \epsilon_{\text{R}}$  between the extinction coefficient  $\epsilon_{\text{P}}$  of the products  $[\text{Fe}^{\text{III}}_7\text{Fe}^{\text{II}}(\mu^4\text{-O}_4)(\mu\text{-Pz})_{12}\text{X}_4]^-$  and  $\epsilon_{\text{R}}$  of the  $[\text{Fe}^{\text{III}}_8(\mu^4\text{-O}_4)(\mu\text{-Pz})_{12}\text{X}_4]$  complexes were calculated using the expression  $\epsilon_{\text{P}} - \epsilon_{\text{R}} = \Delta A_{\infty}/[e]_0$ . The absorbance change,  $\Delta A_{\infty}$ , was recorded after the reduction of  $[\text{Fe}^{\text{III}}_8(\mu^4\text{-O}_4)(\mu\text{-Pz})_{12}\text{X}_4]$  was completed and the initial concentration of the reductant,  $[e]_0$ , was the concentration of  $e_{\text{sol}}^-$ ,  $[\text{Ni}^{\text{I}}(\text{Me}_6[14]\text{aneN}_4)]^+$ , and  $[\text{Cr}^{\text{II}}(\text{Me}_6[14]\text{aneN}_4)]^{2+}$  either produced by the radiolytic pulse or produced immediately afterward when the  $e_{\text{sol}}^-$  reacted with the Ni(II) and Cr(III) parent complexes. Values of the extinction coefficients obtained from the reactions of  $e_{\text{sol}}^-$ ,  $[\text{Ni}^{\text{I}}(\text{Me}_6[14]\text{aneN}_4)]^+$ , and  $[\text{Cr}^{\text{II}}(\text{Me}_6[14]\text{aneN}_4)]^{2+}$  differed in less than 5%. Such a small dispersion between the calculated values of  $\epsilon_{\text{P}}$  indicates that the same mixed-valence  $[\text{Fe}^{\text{III}}_7\text{Fe}^{\text{II}}(\mu^4\text{-O}_4)(\mu\text{-Pz})_{12}\text{X}_4]^-$  species was produced in the different reactions and that no error was committed in the evaluation of the products' concentrations.

**LMCT Photochemistry of  $[\text{Fe}^{\text{III}}_8(\mu^4\text{-O}_4)(\mu\text{-Pz})_{12}\text{X}_4]$ .** Continuous photolysis experiments demonstrated the reversibility of the photochemical process of  $[\text{Fe}^{\text{III}}_8(\mu^4\text{-O}_4)(\mu\text{-Pz})_{12}\text{X}_4]^-$  species. Photolysis,  $\lambda_{\text{ex}} = 350$  nm and  $I_{\text{ab}} = 10^{-4}$  Einstein  $\text{L}^{-1} \text{min}^{-1}$ , of a deaerated  $5 \times 10^{-4}$  M  $[\text{Fe}^{\text{III}}_8(\mu^4\text{-O}_4)(\mu\text{-Pz})_{12}\text{Cl}_4]$  solution in  $\text{CH}_3\text{OH}$  for a long period ( $t \sim 3$  h) produced little if any change in the absorption spectrum of the solution. However, large changes in the spectrum of the complex were observed when the irradiated solutions contained  $1.0 \times 10^{-2}$  M NaF. On the basis of the spectra of related clusters,<sup>5,6</sup> the photoinduced spectroscopic changes, i.e., a bleach of the LMCT band and the absence of the spectroscopic features of  $[\text{Fe}^{\text{III}}_7\text{Fe}^{\text{II}}(\mu^4\text{-O}_4)(\mu\text{-Pz})_{12}\text{X}_4]^-$  mixed-valence species, was attributed to the formation of a product,  $[\text{Fe}^{\text{III}}_8(\mu^4\text{-O}_4)(\mu\text{-Pz})_{12}\text{Cl}_3\text{F}]$ . Negligible changes were observed in the UV–vis spectrum of blanks having the same concentrations of complex and NaF but kept



**TABLE 1: Reduction of  $[\text{Fe}^{\text{III}}_8(\mu^4\text{-O}_4)(\mu\text{-Pz})_{12}\text{Cl}_4]$  by Transition Metal Complexes**

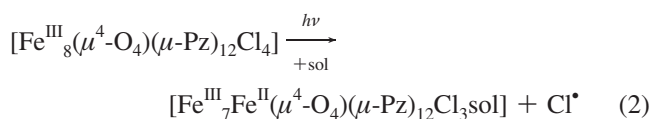
reducing species ( $\text{R}^-$ )	$E^0, {}^a \text{V}$	$k_{\text{R}^+/\text{R}}, {}^a \text{M}^{-1} \text{s}^{-1}$	$k_{\text{cross}}, {}^b \text{M}^{-1} \text{s}^{-1}$	$^*\lambda_{\text{re}} (^*E^0), {}^c \text{kJ mol}^{-1}(\text{V})$
$[\text{Cr}(\text{bpy})_3]^{2+}$	−0.26	$2.0 \times 10^9$	$2.8 \times 10^7$	30.97 (0.250) (d) <sup>c</sup>
$[\text{Cr}(\text{Me}_6[14]\text{aneN}_4)]^{2+}$	−0.72	$10^7$	$8.5 \times 10^8$	31.91 (0.265) (e) <sup>c</sup>
$[\text{Ni}(\text{Me}_6[14]\text{aneN}_4)]^+$	−1.00	$1.2 \times 10^4$	$3.0 \times 10^9$	30.64 (0.264) (f) <sup>c</sup>
$[\text{Rh}(\text{Me}_6[14]\text{aneN}_4)]^{2+}$	−0.92		$1.4 \times 10^9$	

<sup>a</sup> Reduction potentials,  $E^0$ , and self-exchange rate constants,  $k_{\text{R}^+/\text{R}}$ , of the  $\text{R}^+/\text{R}$  couple communicated in the literature.<sup>19–27</sup> <sup>b</sup> Rate constants of the reaction of  $\text{R}^-$  with  $[\text{Fe}^{\text{III}}_8(\mu^4\text{-O}_4)(\mu\text{-Pz})_{12}\text{Cl}_4]$ . <sup>c</sup> Calculated reorganization energies  $^*\lambda_{\text{re}}$  of the self-exchange reaction, eq 11, and the standard potential  $^*E^0$  of the couple  $[\text{Fe}^{\text{III}}_8(\mu^4\text{-O}_4)(\mu\text{-Pz})_{12}\text{Cl}_4]/[\text{Fe}^{\text{III}}_7\text{Fe}^{\text{II}}(\mu^4\text{-O}_4)(\mu\text{-Pz})_{12}\text{Cl}_4]^-$ . Results obtained using systems of two quadratic equations with the data of a pair of reactions: (d)  $[\text{Fe}^{\text{III}}_8(\mu^4\text{-O}_4)(\mu\text{-Pz})_{12}\text{Cl}_4]$  with  $[\text{Cr}(\text{bpy})_3]^{2+}$  and  $[\text{Cr}(\text{Me}_6[14]\text{aneN}_4)]^{2+}$ , (e)  $[\text{Fe}^{\text{III}}_8(\mu^4\text{-O}_4)(\mu\text{-Pz})_{12}\text{Cl}_4]$  with  $[\text{Cr}(\text{bpy})_3]^{2+}$  and  $[\text{Ni}(\text{Me}_6[14]\text{aneN}_4)]^+$ , and (f)  $[\text{Fe}^{\text{III}}_8(\mu^4\text{-O}_4)(\mu\text{-Pz})_{12}\text{Cl}_4]$  with  $[\text{Cr}(\text{Me}_6[14]\text{aneN}_4)]^{2+}$  and  $[\text{Ni}(\text{Me}_6[14]\text{aneN}_4)]^+$ .

in the dark for the same periods of the photolysis. This experimental observation shows that thermal ligand-substitution reactions are much slower than the photoinduced processes.

The formation of the  $[\text{Fe}^{\text{III}}_8(\mu^4\text{-O}_4)(\mu\text{-Pz})_{12}\text{Cl}_3\text{F}]$  product in the presence of NaF can be attributed either to a photoinduced ligand substitution or to back redox reactions of the products formed in a photoredox process. To distinguish between these two processes, ethylene,  $\text{CH}_2\text{CH}_2$ , was used as a scavenger of the radicals that are expected to be produced by a photoredox process and to change, in the case photoredox process, the photolysis course. A bleach of the solution's spectrum at wavelengths of the LMCT absorption band was observed during the 350 nm photolysis of  $5 \times 10^{-4} \text{ M}$   $[\text{Fe}^{\text{III}}_8(\mu^4\text{-O}_4)(\mu\text{-Pz})_{12}\text{Cl}_4]$  in  $\text{CH}_2\text{CH}_2$ -saturated  $\text{CH}_3\text{OH}$  and the amount of bleach increased with the irradiation time. Hence, the photoinduced changes in the UV–vis spectrum of the solution in the presence of NaF or  $\text{CH}_2\text{CH}_2$  must be associated with photoredox reactions rather than a photoinduced ligand substitution. The  $[\text{Fe}^{\text{III}}_8(\mu^4\text{-O}_4)(\mu\text{-Pz})_{12}\text{Br}_4]$  displayed the same photoreversible behavior of  $[\text{Fe}^{\text{III}}_8(\mu^4\text{-O}_4)(\mu\text{-Pz})_{12}\text{Cl}_4]$  due to a back redox reaction of the photoproducts, e.g.,  $[\text{Fe}^{\text{III}}_7\text{Fe}^{\text{II}}(\mu^4\text{-O}_4)(\mu\text{-Pz})_{12}\text{Br}_3\text{sol}]$  where S = solvent and  $\text{Br}^\bullet$ . These experimental observations were confirmed using the flash photolysis technique.

**Mixed-Valence Photoproducts.** The photoreversibility exhibited by  $[\text{Fe}^{\text{III}}_8(\mu^4\text{-O}_4)(\mu\text{-Pz})_{12}\text{X}_4]$  in the absence of scavengers gives an indication of back reactions between the photogenerated species. To investigate the existence of such transient species in the photolyzed solutions,  $10^{-3}$  to  $10^{-4} \text{ M}$   $[\text{Fe}^{\text{III}}_8(\mu^4\text{-O}_4)(\mu\text{-Pz})_{12}\text{Cl}_4]$  in deaerated  $\text{CH}_3\text{OH}$  or  $\text{CH}_3\text{CN}$  was flash irradiated at 351 nm. Photoinduced changes in the absorption spectrum were followed in a 15 ns to millisecond time domain. The irradiation of the solution bleaches the MLCT absorption band at  $\lambda_{\text{max}} < 400 \text{ nm}$  and increases the absorbance of the solution at  $\lambda_{\text{ob}} > 500 \text{ nm}$  during the 15 ns duration of the flash, Figure 3. The photoinduced changes of the absorption spectrum are consistent with the formation of the product  $[\text{Fe}^{\text{III}}_7\text{Fe}^{\text{II}}(\mu^4\text{-O}_4)(\mu\text{-Pz})_{12}\text{X}_3\text{sol}]$  (sol =  $\text{CH}_3\text{OH}$  or  $\text{CH}_3\text{CN}$ ) and a concomitant generation of  $\text{Cl}^\bullet$  radicals, eq 2.



A comparison of the traces recorded at  $\lambda_{\text{ob}} = 540$  and 375 nm, Figure 3, reveals that the decay of the 540 nm absorbance is faster,  $t_{1/2} = 69 \text{ ns}$  and  $\Delta A = 1.6 \times 10^{-3}$ , than the recovery of the 375 nm absorbance,  $t_{1/2} = 400 \text{ ns}$  and  $\Delta A = -1.8 \times 10^{-3}$ . The spectra recorded after the flash irradiation of  $[\text{Fe}^{\text{III}}_8(\mu^4\text{-O}_4)(\mu\text{-Pz})_{12}\text{Cl}_4]$  and the pulse radiolysis generated  $[\text{Fe}^{\text{III}}_7\text{Fe}^{\text{II}}(\mu^4\text{-O}_4)(\mu\text{-Pz})_{12}\text{X}_4]^-$  exhibited similar features. Because of the dissociative nature of the photolytic process, the increase of the

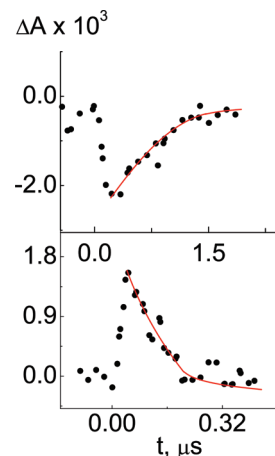
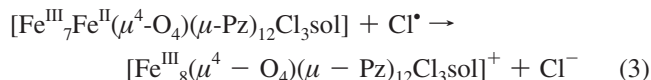
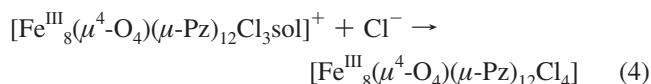


**Figure 3.** Oscillographic traces recorded in the 351 nm flash irradiation of  $10^{-4} \text{ M}$   $[\text{Fe}^{\text{III}}_8(\mu^4\text{-O}_4)(\mu\text{-Pz})_{12}\text{Cl}_4]$  in deaerated  $\text{CH}_3\text{CN}$ : top,  $\lambda_{\text{ob}} = 375 \text{ nm}$ ; bottom,  $\lambda_{\text{ob}} = 540 \text{ nm}$ .

540 nm absorbance was attributed to the formation of  $[\text{Fe}^{\text{III}}_7\text{Fe}^{\text{II}}(\mu^4\text{-O}_4)(\mu\text{-Pz})_{12}\text{X}_3\text{sol}]$  and the fastest process to the outer-sphere oxidation of the  $\text{Fe}(\text{II})$  product, eq 3.



Equation 3 is consistent with the disappearance of the spectroscopic features at  $\lambda_{\text{ob}} > 500 \text{ nm}$  that were ascribed to the mixed-valence complex. In addition, the slowest process regenerates the spectrum of the solution, i.e., the spectrum recorded prior to the flash irradiation. On this basis, the last change of the photogenerated spectrum must be caused by the anation of the oxidized product, eq 4.



The dependence of the rate of the 375 nm absorbance recovery on the  $[\text{Fe}^{\text{III}}_7\text{Fe}^{\text{II}}(\mu^4\text{-O}_4)(\mu\text{-Pz})_{12}\text{X}_3\text{sol}]$  concentration has shown that the process is kinetically of second order on the concentration of the latter. In this study, various  $[\text{Fe}^{\text{III}}_7\text{Fe}^{\text{II}}(\mu^4\text{-O}_4)(\mu\text{-Pz})_{12}\text{X}_3\text{sol}]$  concentrations were obtained by the irradiation of the solutions with Figure 4c laser powers. A ratio of the second-order rate constant to the extinction coefficients,  $k/\epsilon \sim 6 \times 10^8 \text{ cm}^2 \text{s}^{-1}$  at 375 nm, was calculated from the oscillographic traces recorded under these conditions.

Flash photolysis experiments also confirmed the formation of  $\text{Cl}^\bullet$  via eq 2. Since  $\text{Cl}^\bullet$  radicals are complexed by  $\text{Cl}^-$  to form  $\text{Cl}_2^{\bullet-}$ , a deaerated solution of  $1 \times 10^{-4} \text{ M}$   $[\text{Fe}^{\text{III}}_8(\mu^4\text{-O}_4)(\mu\text{-Pz})_{12}\text{Cl}_4]$

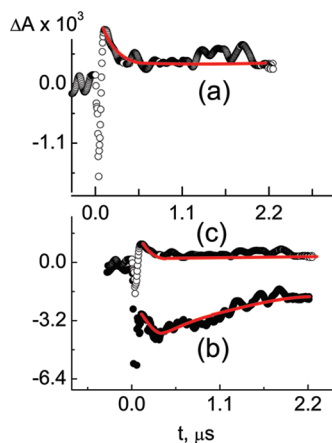


**Figure 4.** Oscillographic traces recorded in the 351 nm flash irradiation of  $10^{-4}$  M  $[\text{Fe}^{\text{III}}_8(\mu^4\text{-O}_4)(\mu\text{-Pz})_{12}\text{Cl}_4]$  in deaerated  $\text{CH}_3\text{CN}$  containing  $10^{-2}$  M TBAI (a,  $\lambda_{\text{ob}} = 400$  nm) or saturated in  $\text{CH}_2\text{CH}_2$  (b,  $\lambda_{\text{ob}} = 580$  nm and, c,  $\lambda_{\text{ob}} = 400$  nm).

$\text{Pz})_{12}\text{Cl}_4]$  and  $10^{-2}$  M TBACl was flash irradiated at 351 nm. The flash irradiation produced a small increase of the absorbance at  $\lambda_{\text{ob}} < 400$  nm, consistent with the photogeneration of  $\text{Cl}_2^{\bullet-}$ .<sup>18</sup> Moreover, the formation of  $\text{Cl}^\bullet$  radicals via eq 2 was confirmed using the radical scavengers, TBAI and  $\text{CH}_2\text{CH}_2$ , in different solutions of  $[\text{Fe}^{\text{III}}_8(\mu^4\text{-O}_4)(\mu\text{-Pz})_{12}\text{Cl}_4]$ . The formation of  $\text{I}_2^{\bullet-}$  when a solution containing  $10^{-2}$  M TBAI and  $10^{-4}$  M  $[\text{Fe}^{\text{III}}_8(\mu^4\text{-O}_4)(\mu\text{-Pz})_{12}\text{Cl}_4]$  was flash photolyzed at 351 nm was confirmed by the fast increase of the solution absorbance in the near UV region of the spectrum.<sup>18</sup> Such a growth of the solution's absorbance is due to the oxidation  $\text{I}^-$  by  $\text{Cl}^\bullet$  radicals and the subsequent formation of  $\text{I}_2^{\bullet-}$  in the presence of  $\text{I}^-$ . The decay of  $\text{I}_2^{\bullet-}$  was followed at 400 nm, Figure 4a, and it is attributed to the reaction of the  $\text{I}_2^{\bullet-}$  radicals with  $[\text{Fe}^{\text{III}}_7\text{Fe}^{\text{II}}(\mu^4\text{-O}_4)(\mu\text{-Pz})_{12}\text{Cl}_3\text{sol}]$ . Both the dependence of the reaction rate on the concentration of  $\text{I}_2^{\bullet-}$  and the least-squares fitting of the oscillographic traces showed that the latter reaction is kinetically of second order. A quotient of the rate constant to the extinction coefficients,  $k/\Sigma\epsilon \sim 2.5 \times 10^7 \text{ cm s}^{-1}$  at 400 nm, was calculated for the reaction of  $\text{I}_2^{\bullet-}$  radicals with  $[\text{Fe}^{\text{III}}_7\text{Fe}^{\text{II}}(\mu^4\text{-O}_4)(\mu\text{-Pz})_{12}\text{Cl}_3\text{sol}]$ . Ethylene,  $\text{CH}_2\text{CH}_2$ , was also used as a scavenger of  $\text{Cl}^\bullet$  radicals. Flash irradiation of a  $10^{-4}$  M  $[\text{Fe}^{\text{III}}_8(\mu^4\text{-O}_4)(\mu\text{-Pz})_{12}\text{Cl}_4]$  saturated with  $\text{CH}_2\text{CH}_2$  produces a bleach of the 400 nm absorbance, Figure 4b,c, within the duration of the flash. A further bleach of the 400 nm absorbance takes place with  $t_{1/2} \sim 200$  ns. Inspection of the irradiated solution at 580 nm, Figure 4b, reveals transient changes of the absorbance in the same time scale of the processes observed at  $\lambda_{\text{ob}} = 400$  nm, Figure 4c. In contrast to the photolysis in the absence of scavengers, Figure 3, the recovery of the 400 nm absorbance ( $t_{1/2} \sim 700$  ns, Figure 4) in the presence of  $\text{CH}_2\text{CH}_2$  is incomplete because the  $\text{Cl}^\bullet$  radicals produced via eq 2 are trapped by  $\text{CH}_2\text{CH}_2$ , eq 5.



Because of the trapping of the  $\text{Cl}^\bullet$  by  $\text{CH}_2\text{CH}_2$ , eq 5,  $\text{Cl}^\bullet$  cannot be formed via eq 3 in a stoichiometric concentration, i.e., the concentration required for a quantitative regeneration of the  $[\text{Fe}^{\text{III}}_8(\mu^4\text{-O}_4)(\mu\text{-Pz})_{12}\text{Cl}_4]$  complex, eq 4. Indeed, a fraction of the bleach of the solution, e.g., at  $\lambda_{\text{ob}} = 380$  nm, remains at the end of the trace shown in Figure 4b. The residual 580 nm absorbance remaining at the end of the trace in Figure 4c shows that a back-reaction between  $\text{ClCH}_2\text{C}^\bullet\text{H}_2$  and  $[\text{Fe}^{\text{III}}_7\text{Fe}^{\text{II}}(\mu^4\text{-O}_4)(\mu\text{-Pz})_{12}\text{Cl}_3\text{sol}]$  forms products different from the product of eq 3,

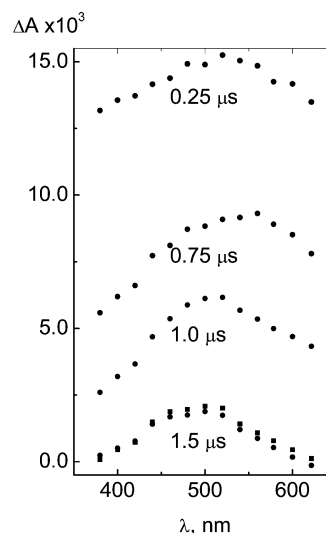
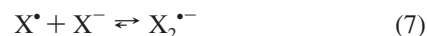
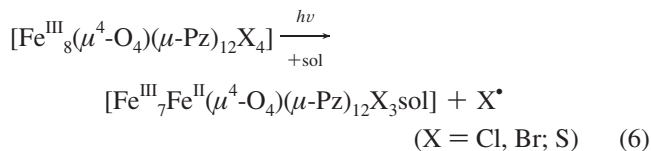


**Figure 5.** Transient spectra recorded in the 351 nm flash irradiation of  $1.0 \times 10^{-5}$  M  $[\text{Fe}^{\text{III}}_8(\mu^4\text{-O}_4)(\mu\text{-Pz})_{12}\text{Br}_4]$  in deaerated  $\text{CH}_3\text{OH}$  containing  $1.0 \times 10^{-3}$  M TBABr.

i.e.,  $[\text{Fe}^{\text{III}}_8(\mu^4\text{-O}_4)(\mu\text{-Pz})_{12}\text{Cl}_3\text{sol}]^+$ . For example, some  $[\text{Fe}^{\text{III}}_7\text{Fe}^{\text{II}}(\mu^4\text{-O}_4)(\mu\text{-Pz})_{12}\text{Cl}_3\text{sol}]$  could have been left at the end of the reaction. This will be the case if the reoxidation of  $[\text{Fe}^{\text{III}}_7\text{Fe}^{\text{II}}(\mu^4\text{-O}_4)(\mu\text{-Pz})_{12}\text{Cl}_3\text{sol}]$  by C-centered radicals, i.e.,  $\text{ClCH}_2\text{C}^\bullet\text{H}_2$  radicals and radicals produced by the  $\text{CH}_2\text{CH}_2$  polymerization, has to compete with the bimolecular radical–radical terminations of the C-centered radicals.

Similar flash photochemical studies were carried out with solutions of  $[\text{Fe}^{\text{III}}_8(\mu^4\text{-O}_4)(\mu\text{-Pz})_{12}\text{Br}_4]$  in deaerated  $\text{CH}_3\text{OH}$ . The 351 nm flash irradiation of  $1.0 \times 10^{-5}$  M  $[\text{Fe}^{\text{III}}_8(\mu^4\text{-O}_4)(\mu\text{-Pz})_{12}\text{Br}_4]$  in deaerated  $\text{CH}_3\text{OH}$  containing  $1.0 \times 10^{-3}$  M TBABr produced transient spectra with  $\lambda_{\text{max}} = 520$  nm, Figure 5. A comparison of the spectra in Figure 3 with the spectrum of the reduced complex produced in pulse radiolysis experiments described above and the spectrum of  $\text{Br}_2^{\bullet-}$  suggests that the spectra in Figure 5 must be assigned to a convolution of the spectra of the two species. A ratio of the second-order rate constant to the sum of extinction coefficients,  $k/\Sigma\epsilon \sim 4.3 \times 10^6 \text{ cm s}^{-1}$  at 400 nm, was calculated for the decay of the photogenerated species. On the basis of this assignment, the  $[\text{Fe}^{\text{III}}_8(\mu^4\text{-O}_4)(\mu\text{-Pz})_{12}\text{Cl}_4]$  and  $[\text{Fe}^{\text{III}}_8(\mu^4\text{-O}_4)(\mu\text{-Pz})_{12}\text{Br}_4]$  complexes must have a similar photoredox behavior, which is summarized by eqs 6 and 7.

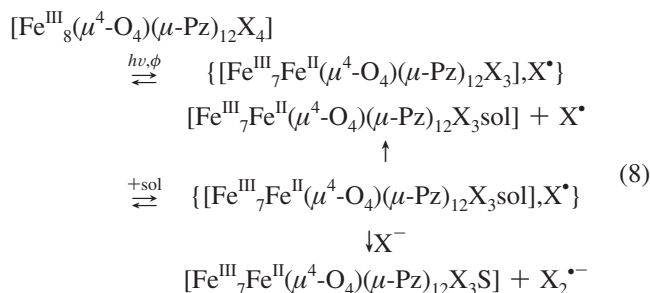


Quantum yields of the  $[\text{Fe}^{\text{III}}_8(\mu^4\text{-O}_4)(\mu\text{-Pz})_{12}\text{X}_4]$  photoprocesses, Table 2, were calculated using the photogenerated concentrations of  $\text{X}_2^{\bullet-}$  radicals,  $[\text{X}_2^{\bullet-}] = \Delta A/(\epsilon_{\text{X}_2^{\bullet-}} + \epsilon_{\text{P}} - \epsilon_{\text{R}})$  where  $\Delta A$  is the absorbance change at 350 nm and  $\epsilon_{\text{P}} - \epsilon_{\text{R}} \sim 4 \times 10^3 \text{ M}^{-1} \text{ cm}^{-1}$ . To trap quantitatively the  $\text{X}^\bullet$  radicals, the chloride and bromide complexes were flash irradiated at 351 nm in deaerated methanol containing respectively  $10^{-1}$  M TBACl and  $10^{-1}$  M TBABr. The quantum yield of  $\text{Cl}_2^{\bullet-}$ ,  $\Phi_{\text{X}_2^{\bullet-}}$

**TABLE 2: Quantum Yields of the Product Formation and Ratio of the Escape vs Recombination of the Photoproducts**

photolyte	$\Phi_{X_2^-}$	$\Phi$	$\rho_{\text{escape}}/\rho_{\text{recombination}}$
$[\text{Fe}^{\text{III}}_8(\mu^4\text{-O}_4)(\mu\text{-Pz})_{12}\text{Cl}_4]$	$(6.3 \pm 0.6) \times 10^{-2}$	$(5.3 \pm 0.6) \times 10^{-3}$	$9.1 \times 10^{-2}$
$[\text{Fe}^{\text{III}}_8(\mu^4\text{-O}_4)(\mu\text{-Pz})_{12}\text{Br}_4]$	$(2.8 \pm 0.1) \times 10^{-1}$	$(2.1 \pm 0.4) \times 10^{-2}$	$8.6 \times 10^{-2}$

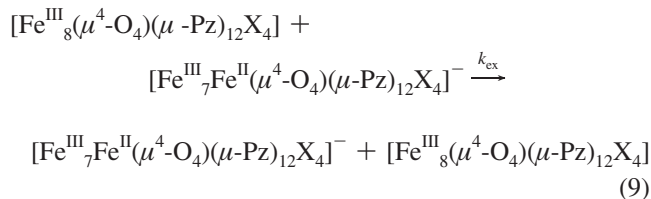
$= (6.3 \pm 0.6) \times 10^{-2}$ , was considerably smaller than the quantum yield of  $\text{Br}_2^{\bullet-}$ ,  $\Phi_{X_2^-} = (2.8 \pm 0.1) \times 10^{-1}$ . Also, product concentrations were calculated in the absence of added halide using for the calculation the amount of the 350 nm absorbance bleached and the corresponding extinction coefficients of the parent and product complexes. A comparison of the quantum yields, Table 2, reveals that there is near 1 order of magnitude difference between the quantum yields calculated in the absence of halide, i.e.,  $\Phi = (5.3 \pm 0.6) \times 10^{-3}$  for the chloride complex and  $\Phi = (2.1 \pm 0.4) \times 10^{-2}$  for the bromide complex, and those calculated for the  $X_2^{\bullet-}$  radicals. The difference between  $\Phi_{X_2^-}$  and  $\Phi$  is much larger than the uncertainties in the value of  $\epsilon_R$ , and it must be attributed to the recombination of  $X^\bullet$  radicals with the metallo fragment. This is shown in eq 8 where  $X^-$  traps  $X^\bullet$  radicals in the solvent cage in competition with the recombination of the photofragments.<sup>28a</sup>



A  $\sim 9 \times 10^{-2}$  ratio of the probability of overall photoproduct escape from the geminate pair to the probability of the recombination, Table 2, was estimated on the basis of the mechanism in eq 8.

**Analysis of Experimental Observations.** Because the one-electron reduction of the  $[\text{Fe}^{\text{III}}_8(\mu^4\text{-O}_4)(\mu\text{-Pz})_{12}\text{X}_4]$  ( $X = \text{Cl}, \text{Br}$ ) complexes leaves the outer Fe(III) sites unaffected,<sup>9</sup> the redox active  $\text{Fe}_4\text{O}_4$  cubane core is the primary acceptor of electrons in the thermal reduction of  $[\text{Fe}^{\text{III}}_8(\mu^4\text{-O}_4)(\mu\text{-Pz})_{12}\text{Cl}_4]$  by reductants having redox potentials  $E^0 \geq -1.0$  V vs NHE, Table 1. These reactions differ with the  $e^-_{\text{sol}}$  reaction where a metastable product,  $[\text{Fe}^{\text{III}}_7\text{Fe}^{\text{II}}(\mu^4\text{-O}_4)(\mu\text{-Pz})_{12}\text{X}_4]^-$ , is formed in the reduction process, eq 1. This product can be one where a Fe(III) in the outer shell has been reduced by  $e^-_{\text{sol}}$ . The necessary driving force for the reduction of an outer Fe(III) must be provided by the very negative reduction potential of the  $e^-_{\text{sol}}$ , i.e.,  $E^0 \sim -2.75$  V vs NHE. Electrochemical experiments suggest that the potential for the reduction of this type of Fe(III) in  $[\text{Fe}^{\text{III}}_8(\mu^4\text{-O}_4)(\mu\text{-Pz})_{12}\text{Cl}_4]$  is  $E^0 \leq -1.0$  V vs NHE, i.e., more negative than the reduction potentials of the  $R^-$  species.

The reactions of  $R^-$  with  $[\text{Fe}^{\text{III}}_8(\mu^4\text{-O}_4)(\mu\text{-Pz})_{12}\text{Cl}_4]$  are outer-sphere electron transfers whose rate constants, Table 1, should have values close to those calculated with the Marcus. On this presumption, a reorganization energy,  $\lambda_{\text{re}} = (2.2 \pm 0.3) \times 10^2$  kJ mol<sup>-1</sup>, of the self-exchange  $[\text{Fe}^{\text{III}}_8(\mu^4\text{-O}_4)(\mu\text{-Pz})_{12}\text{X}_4]/[\text{Fe}^{\text{III}}_7\text{Fe}^{\text{II}}(\mu^4\text{-O}_4)(\mu\text{-Pz})_{12}\text{X}_4]^-$ , eq 9

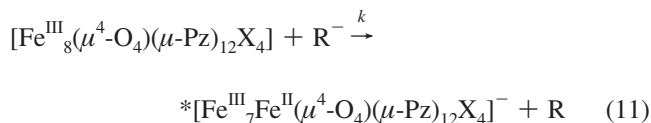


The  $\lambda_{\text{re}}$  was calculated using the expression,  $k_{\text{ex}} = 10^{11} \times \exp(-\lambda_{\text{re}}/4RT)$ , where  $k_{\text{ex}}$  is the self-exchange rate constant.<sup>25-27</sup> Values of  $k_{\text{ex}}$  were calculated using the rate constants of the cross reactions,  $k_{\text{cross}}$ , shown in Table 1 and the Marcus derived expression of the cross-reaction rate constant.<sup>25-27</sup> The values of  $\lambda_{\text{re}}$ , Table 1, are extraordinarily large. Indeed,  $\lambda_{\text{re}}$  regarded as the summation of the outer sphere,  $\lambda_{\text{re,o}}$ , and inner sphere,  $\lambda_{\text{re,i}}$ , reorganization energies, i.e.,  $\lambda_{\text{re}} = \lambda_{\text{re,o}} + \lambda_{\text{re,i}}$ , receives only a small contribution from the outer sphere reorganization energy,  $\lambda_{\text{re,o}} \sim 6.5$  kJ mol<sup>-1</sup>. This energy was calculated using the expression  $\lambda_{\text{re,o}} = (\Delta e)^2/2r(1/n^2 - 1/D)$  with radii  $r \sim 6$  Å for both reactants and the refractive index,  $n \sim 1.33$ , of MeOH. Because bond angles and bond lengths in the crystallographic structures of  $[\text{Fe}^{\text{III}}_8(\mu^4\text{-O}_4)(\mu\text{-Pz})_{12}\text{X}_4]$  and  $[\text{Fe}^{\text{III}}_7\text{Fe}^{\text{II}}(\mu^4\text{-O}_4)(\mu\text{-Pz})_{12}\text{X}_4]^-$  are nearly identical,<sup>9</sup> the inner sphere reorganization energy, eq 10, must be insignificant.

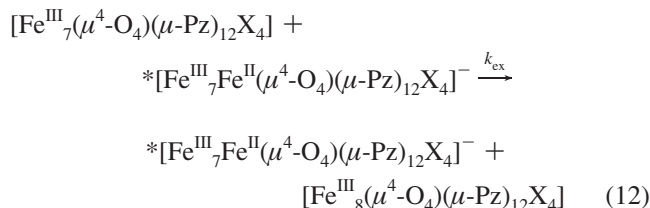
$$\lambda_{\text{re,i}} = \sum [f_n^{\text{r}} f_n^{\text{p}} / f_n^{\text{r}} + f_n^{\text{p}}] \delta q_n^2 \quad (10)$$

In eq 10,  $f_n^{\text{r}}$  and  $f_n^{\text{p}}$  are respectively the force constants of the  $n$ th normal mode of the reactant and product and  $\delta q_n \sim 0$  is the difference in the equilibrium distances of the  $n$ th normal mode of the reactant and product. Because  $\lambda_{\text{re,i}} \sim 0$ , there is a difference,  $\lambda_{\text{re}} - \lambda_{\text{re,o}} = 2.1 \times 10^2$  kJ mol<sup>-1</sup>, that cannot be accounted for on the basis of the self-exchange reaction described in eq 9.

To account for the experimental results, the inner sphere reorganization energy must be  $\sim 2.1 \times 10^2$  kJ mol<sup>-1</sup>.  $[\text{Fe}^{\text{III}}_7\text{Fe}^{\text{II}}(\mu^4\text{-O}_4)(\mu\text{-Pz})_{12}\text{X}_4]^-$  must be therefore a secondary product of the electron transfer reactions with  $R^-$ . It is possible to explain such a large reorganization energy if it is assumed that the electron transfer reactions investigated in this work generate a product  $*[\text{Fe}^{\text{III}}_7\text{Fe}^{\text{II}}(\mu^4\text{-O}_4)(\mu\text{-Pz})_{12}\text{Cl}_4]^-$ , eq 11.



The product of eq 11,  $*[\text{Fe}^{\text{III}}_7\text{Fe}^{\text{II}}(\mu^4\text{-O}_4)(\mu\text{-Pz})_{12}\text{Cl}_4]^-$ , is different from the product of the electrochemical reduction,  $[\text{Fe}^{\text{III}}_7\text{Fe}^{\text{II}}(\mu^4\text{-O}_4)(\mu\text{-Pz})_{12}\text{Cl}_4]^-$ , and  $R^-$  is one of the transition metal complexes in Table 1. Because of the structural differences, the redox potential,  $*E^0$ , of the  $[\text{Fe}^{\text{III}}_8(\mu^4\text{-O}_4)(\mu\text{-Pz})_{12}\text{Cl}_4]/*[\text{Fe}^{\text{III}}_7\text{Fe}^{\text{II}}(\mu^4\text{-O}_4)(\mu\text{-Pz})_{12}\text{Cl}_4]^-$  couple and the reorganization energy  $*\lambda_{\text{re}}$  of eq 12, both unknowns, were calculated by solving a set of two nonlinear equations.<sup>25a</sup>

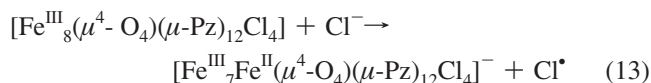


Each quadratic equation resulted from expanding the corrected Marcus equation for the rate constant of the cross reaction,<sup>25</sup> and the set was made with the data of two cross reactions in Table 1. It is worth mentioning the agreement between the results obtained from three different combinations of the experimental data in Table 1. It confirms that the reactions proceed via an outer sphere transfer of electrons. The treatment yields the average values  $*E^0 = 0.26 \pm 0.01$  V vs NHE,  $*\lambda_{\text{re}} = 30.5 \pm 0.5$  kJ mol<sup>-1</sup>, and  $*\lambda_{\text{re,i}} = *\lambda_{\text{re}} - \lambda_{\text{re,o}} \sim 24$  kJ mol<sup>-1</sup>. Substituting in eq 9 the values of  $*\lambda_{\text{re,i}}$  and the Fe–O stretching frequency communicated for  $[\text{Fe}^{\text{III}}_8(\mu^4\text{-O}_4)(\mu\text{-Pz})_{12}\text{Cl}_4]$  and  $*[\text{Fe}^{\text{III}}_7\text{Fe}^{\text{II}}(\mu^4\text{-O}_4)(\mu\text{-Pz})_{12}\text{Cl}_4]^-$  complexes,<sup>5,6</sup> we assumed a difference between the Fe–O bond distances of the reactants in eq 12,  $\delta q_n \sim 0.16$  Å.

The species  $*[\text{Fe}^{\text{III}}_7\text{Fe}^{\text{II}}(\mu^4\text{-O}_4)(\mu\text{-Pz})_{12}\text{Cl}_4]^-$  can be a short-lived excited state of  $[\text{Fe}^{\text{III}}_7\text{Fe}^{\text{II}}(\mu^4\text{-O}_4)(\mu\text{-Pz})_{12}\text{Cl}_4]^-$ , for example, with a different spin multiplicity than the one exhibited by  $[\text{Fe}^{\text{III}}_7\text{Fe}^{\text{II}}(\mu^4\text{-O}_4)(\mu\text{-Pz})_{12}\text{Cl}_4]^-$ . It is highly improbable that  $*[\text{Fe}^{\text{III}}_7\text{Fe}^{\text{II}}(\mu^4\text{-O}_4)(\mu\text{-Pz})_{12}\text{Cl}_4]^-$  is an electronic isomer of  $[\text{Fe}^{\text{III}}_7\text{Fe}^{\text{II}}(\mu^4\text{-O}_4)(\mu\text{-Pz})_{12}\text{Cl}_4]^-$  with an electron in one of the outer Fe ions. Such a species will be similar to the product of the  $[\text{Fe}^{\text{III}}_8(\mu^4\text{-O}_4)(\mu\text{-Pz})_{12}\text{Cl}_4]$  reduction by the solvated electron, namely,  $[\text{Fe}^{\text{III}}_7\text{Fe}^{\text{II}}(\mu^4\text{-O}_4)(\mu\text{-Pz})_{12}\text{X}_4]^-$  in eq 1, which is only produced at a more negative standard potential than those of the reactants R<sup>-</sup>.

Inspection of the absorption spectrum of  $[\text{Fe}^{\text{III}}_7\text{Fe}^{\text{II}}(\mu^4\text{-O}_4)(\mu\text{-Pz})_{12}\text{Cl}_4]^-$  lends some support to the proposition that  $*[\text{Fe}^{\text{III}}_7\text{Fe}^{\text{II}}(\mu^4\text{-O}_4)(\mu\text{-Pz})_{12}\text{Cl}_4]^-$  is a short-lived excited state of the latter species. Indeed, the reorganization energy  $*\lambda_{\text{re}}$  plus the standard potential  $*E^0$  yield an energy close in magnitude to a weak optical transition at  $\lambda_{\text{max}} \sim 1.3 \times 10^4$  cm<sup>-1</sup> in the absorption spectrum of  $[\text{Fe}^{\text{III}}_7\text{Fe}^{\text{II}}(\mu^4\text{-O}_4)(\mu\text{-Pz})_{12}\text{Cl}_4]^-$ .

The reorganization energy  $*\lambda_{\text{re}}$ , combined with other thermochemical parameters give also good estimates of the positions of the optical halide–ligand to metal charge transfer transitions, LMCT<sub>Fe–Cl</sub>, in the spectrum of  $[\text{Fe}^{\text{III}}_8(\mu^4\text{-O}_4)(\mu\text{-Pz})_{12}\text{Cl}_4]$ . In terms of the cycle (a) in Figure 6 the energy,  $E_{\text{hv}}$ , of the LMCT<sub>Fe–Cl</sub> electronic transition can be expressed,<sup>28b</sup>  $E_{\text{hv}} = \Delta G^0_{\text{Fe/Cl}} + *\lambda_{\text{re,i}}/2 + \Delta G^0_{\text{Cl}^- \leftrightarrow \text{Cl}^\bullet} \sim 2.69 \times 10^2$  kJ mol<sup>-1</sup> ( $\equiv 446$  nm), where  $\Delta G^0_{\text{Cl}^- \leftrightarrow \text{Cl}^\bullet}$  is the Gibbs free energy associated with the process of replacing a Cl<sup>-</sup> ligand by Cl<sup>•</sup> and  $\Delta G^0_{\text{Fe/Cl}}$  is the Gibbs free energy of the redox reaction, eq 13.



Values of the  $[\text{Fe}^{\text{III}}_8(\mu^4\text{-O}_4)(\mu\text{-Pz})_{12}\text{Cl}_4]/[\text{Fe}^{\text{III}}_7\text{Fe}^{\text{II}}(\mu^4\text{-O}_4)(\mu\text{-Pz})_{12}\text{Cl}_4]^-$  and Cl<sup>-</sup>/Cl<sup>•</sup> reduction potentials were used for the calculation of  $\Delta G^0_{\text{Fe/Cl}} = -96.5 (E^0_{\text{Fe}^{\text{III}}/\text{Fe}^{\text{II}}} - E^0_{\text{Cl}^-/\text{Cl}^\bullet}) \sim 2.17 \times 10^2$  kJ mol<sup>-1</sup>. The change in free energy from the replacement of a Cl<sup>-</sup> ligand by Cl<sup>•</sup>,  $\Delta G^0_{\text{Cl}^- \leftrightarrow \text{Cl}^\bullet} \sim 1.25 \times 10^2$  kJ mol<sup>-1</sup>, receives contributions from the differences in the solvation free energies and the ligand field stabilization energies of the Fe(III) and Fe(II) lowest energy d orbitals. A similar value for the

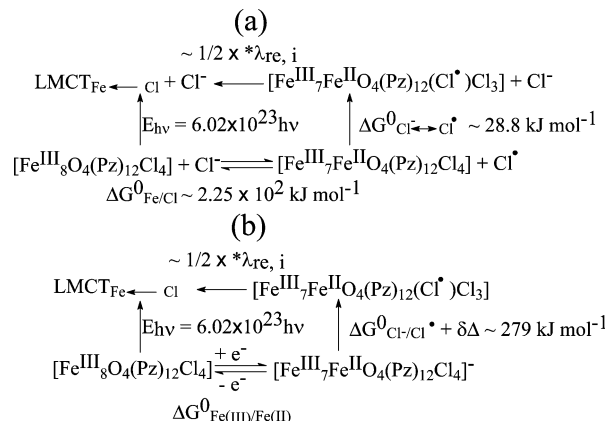


**Figure 6.** Born cycles used for the calculation of the optical LMCT transitions in  $[\text{Fe}^{\text{III}}_8(\mu^4\text{-O}_4)(\mu\text{-Pz})_{12}\text{Cl}_4]$ .

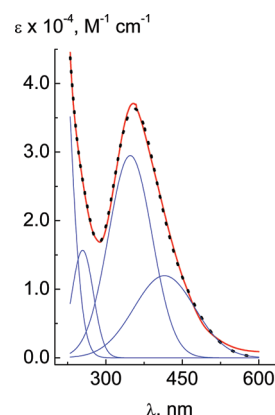


**Figure 7.**  $[\text{Fe}^{\text{III}}_8(\mu^4\text{-O}_4)(\mu\text{-Pz})_{12}\text{Cl}_4]$  spectrum in CH<sub>3</sub>OH (red line) and absorption bands resulting from the multipeak deconvolution of the spectrum (blue lines). The dotted line corresponds to the summation of the bands obtained from the deconvolution treatment.

position of the band,  $E_{\text{hv}} = \Delta G^0_{\text{Fe}^{\text{III}}/\text{Fe}^{\text{II}}} + \Delta G^0_{\text{Cl}^-/\text{Cl}^\bullet} + \delta\Delta + *\lambda_{\text{re,i}}/(2 - 2.64) \times 10^2$  kJ mol<sup>-1</sup> ( $\equiv 450$  nm), was calculated with the cycle (b) in Figure 6. The energies  $\Delta G^0_{\text{Cl}^-/\text{Cl}^\bullet} \sim 2.36 \times 10^2$  kJ mol<sup>-1</sup> and  $\delta\Delta \sim 0.434$  kJ mol<sup>-1</sup> were estimated using the energies of the transitions in the optical spectrum of high spin Fe(III) halide complexes and the angular overlap model expressions in the literature for the energies of these electronic transitions.<sup>29</sup>

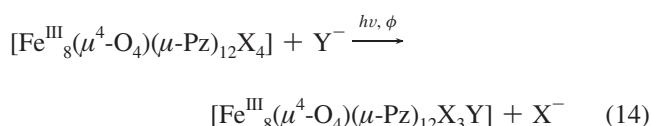
The value of  $E_{\text{hv}}$  ( $\sim 2.64 \times 10^2$  kJ mol<sup>-1</sup>  $\equiv 446$  nm) places the LMCT transition very close to a band with  $\lambda_{\text{max}} = 416$  nm in the multipeak deconvolution of the  $[\text{Fe}^{\text{III}}_8(\mu^4\text{-O}_4)(\mu\text{-Pz})_{12}\text{Cl}_4]$  absorption spectrum, Figure 7. A second band in the absorption spectrum is placed at shorter wavelengths ( $\lambda_{\text{max}} = 349$  nm). If the band with  $\lambda_{\text{max}} = 416$  nm is assigned to an LMCT electronic transition from a  $\pi$  orbital of Cl<sup>-</sup> to the Fe(III), the band with  $\lambda_{\text{max}} = 349$  nm can be assigned to the electronic transition transferring charge from the  $\sigma$  orbital of Cl<sup>-</sup> to Fe(III).<sup>28b</sup> Indeed, the addition of  $\sim 82$  kJ mol<sup>-1</sup> to  $E_{\text{hv}}$ , namely the difference in energy between the  $\pi$  and  $\sigma$  orbitals of Cl<sup>-</sup> estimated on the basis of the Jørgensen's optical electronegativities, places the LMCT transition from the  $\sigma$  orbital of Cl<sup>-</sup> to Fe(III) at  $\sim 344$  nm.

## Discussion

This work has extended the previously established reversibility of electrochemically induced redox processes to photochemically induced redox reactions, e.g., eqs 2–4. Moreover, the photostability of the [Fe<sub>8</sub>] supports the notion that applica-



tions of the photoprocesses are possible. For example, the photoprocess in eq 14, where  $X \neq Y$  condenses and generalizes eq 2–4.



Although many aspects of the photochemistry of these cubanes remain to be investigated over a wide range of wavelengths and a variety of ligands  $\text{X}^-$ , it can be seen that the reversibility of the photoprocesses can be applied to diverse areas, i.e., from catalysis to the preparation of cubanes  $[\text{Fe}^{\text{III}}_8(\mu^4\text{-O}_4)(\mu\text{-Pz})_{12}\text{X}_3\text{Y}]$ . A limit to the latter application is that the photogenerated radical  $\text{X}^\bullet$  must be able to oxidize  $\text{Y}^-$  and the radical  $\text{Y}^\bullet$  must be able to oxidize  $[\text{Fe}^{\text{III}}_7\text{Fe}^{\text{II}}(\mu^4\text{-O}_4)(\mu\text{-Pz})_{12}\text{X}_3\text{sol}]$  in the appropriate time scale.

In addition to the aforementioned potential applications, a number of new mechanistic features of the thermal and photochemical redox processes of  $[\text{Fe}_8]$  cubanes have been uncovered in this work. The reduction of  $[\text{Fe}^{\text{III}}_8(\mu^4\text{-O}_4)(\mu\text{-Pz})_{12}\text{X}_4]$  in MeOH by the  $\text{e}^-_{\text{sol}}$  yields two redox products:  $[\text{Fe}^{\text{III}}_7\text{Fe}^{\text{II}}(\mu^4\text{-O}_4)(\mu\text{-Pz})_{12}\text{Cl}_4]^-$  and  $[\text{Fe}^{\text{III}}_7\text{Fe}^{\text{II}}(\mu^4\text{-O}_4)(\mu\text{-Pz})_{12}\text{Cl}_4]^-$ , the former, a metastable product with a short lifetime, and the latter, the thermodynamically most stable product. Rate constants of a  $10^{10} \text{ M}^{-1} \text{ s}^{-1}$  order of magnitude show that the reductions of the cluster by the  $\text{e}^-_{\text{sol}}$  are diffusion controlled. On the other hand, an intermediate,  $*[\text{Fe}^{\text{III}}_7\text{Fe}^{\text{II}}(\mu^4\text{-O}_4)(\mu\text{-Pz})_{12}\text{Cl}_4]^-$ , unlikely similar to  $[\text{Fe}^{\text{III}}_7\text{Fe}^{\text{II}}(\mu^4\text{-O}_4)(\mu\text{-Pz})_{12}\text{Cl}_4]^-$ , must be postulated to rationalize the rates of the slower reactions between the cluster and transition metal complexes. On the basis of the low spin-crossover energy of  $\text{Fe}(\text{II})$  complexes, an excited state is a possible assignment of  $*[\text{Fe}^{\text{III}}_7\text{Fe}^{\text{II}}(\mu^4\text{-O}_4)(\mu\text{-Pz})_{12}\text{Cl}_4]^-$  and  $[\text{Fe}^{\text{III}}_7\text{Fe}^{\text{II}}(\mu^4\text{-O}_4)(\mu\text{-Pz})_{12}\text{Cl}_4]^-$ .<sup>30–33</sup> The lifetime of the conversion of  $[\text{Fe}^{\text{III}}_7\text{Fe}^{\text{II}}(\mu^4\text{-O}_4)(\mu\text{-Pz})_{12}\text{Cl}_4]^-$  to  $[\text{Fe}^{\text{III}}_7\text{Fe}^{\text{II}}(\mu^4\text{-O}_4)(\mu\text{-Pz})_{12}\text{Cl}_4]^-$  is  $\tau \approx 5 \mu\text{s}$  and it is not unreasonable for a crossover process. However, to ascertain without question the natures of  $*[\text{Fe}^{\text{III}}_7\text{Fe}^{\text{II}}(\mu^4\text{-O}_4)(\mu\text{-Pz})_{12}\text{Cl}_4]^-$  and  $[\text{Fe}^{\text{III}}_7\text{Fe}^{\text{II}}(\mu^4\text{-O}_4)(\mu\text{-Pz})_{12}\text{Cl}_4]^-$ , a much broader study of the redox reactions of related iron cubane complexes will be necessary.

The charge transfer photochemistry of the cubanes is consistent with expectations based on these compounds UV–vis spectroscopy. It is also evident that in the photolysis of the cubanes at  $\lambda_{\text{ex}} \approx 350 \text{ nm}$ , recombination of the photofragments limits the product yields. Moreover, the rationalization of the charge transfer spectroscopy of the  $[\text{Fe}^{\text{III}}_8(\mu^4\text{-O}_4)(\mu\text{-Pz})_{12}\text{X}_4]$  on the basis of parameters derived from the electron transfer reactions confirms that the outer sphere nature of the electron transfer process.

**Acknowledgment.** The support from the Office of Basic Energy Sciences of the U.S. Department of Energy (G.F.), the National Science Foundation, CHE-0822600 (R.G.R.), and the National Institutes of Health, RISE Doctoral Scholarship 2-R25-GM6-1151 (D.P.) are kindly acknowledged. This is contribution No. NDRL-4830 from the Notre Dame Radiation Laboratory.

## References and Notes

- Theil, E. C.; Raymond, K. N. In *Bioinorganic Chemistry*; Bertini, I., Gray, H. B., Lippard, S. J., Selverstone Valentine, J., Eds.; University Science Books: Mill Valley, CA, 1994; pp 1–35.
- Beinert, H.; Holm, R. H.; Münck, E. *Science* **1997**, *277*, 653.
- Rao, P. V.; Holm, R. H. *Chem. Rev.* **2004**, *104*, 527.
- Oshio, H.; Hoshino, N.; Ito, T.; Nakano, M. *J. Am. Chem. Soc.* **2004**, *126*, 8805.
- Raptis, R. G.; Georgakaki, I. P.; Hockless, D. C. R. *Angew. Chem., Int. Ed.* **1999**, *38*, 1632.
- Baran, P.; Boča, R.; Chakraborty, I.; Giapintzakis, J.; Herchel, R.; Huang, O.; McGrady, J. E.; Raptis, R. G.; Sanakis, Y.; Simopoulos, A. *Inorg. Chem.* **2008**, *47*, 645.
- Brimblecombe, R.; Swiegers, G. F.; Dismukes, G. C.; Spiccia, L. *Angew. Chem., Int. Ed.* **2008**, *47*, 7335.
- Narita, K.; Kuwabaza, T.; Sone, K.; Shimizu, K.; Yagi, M. *J. Phys. Chem. B* **2006**, *110*, 23107.
- Chakraborty, I.; Baran, P.; Sanakis, Y.; Simopoulos, A.; Fachini, E.; Raptis, R. G. *Inorg. Chem.* **2008**, *47*, 11734.
- Guerrero, J.; Piro, O. E.; Wolcan, E.; Feliz, M. R.; Ferraudi, G.; Moya, S. A. *Organometallics* **2001**, *20*, 2842.
- Hatchard, C. G.; Parker, C. A. *Proc. R. Soc. London, Ser. A* **1956**, *235*, 518.
- Hugh, G. L.; Wang, Y.; Schöneich, C.; Jiang, P.-Y.; Fesenden, R. W. *Radiat. Phys. Chem.* **1999**, *54*, 559.
- Buxton, G. V.; Greenstock, C. L.; Hellman, W. P.; Ross, A. B. *J. Phys. Chem. Ref. Data* **1988**, *17*, 513.
- Getoff, N.; Ritter, A.; Schworer, F. *Radiat. Phys. Chem.* **1993**, *41*, 797.
- Dorfman, L. M. In *The Solvated Electron in Organic Liquids*, *Adv. Chem. Series*; Gould, R. F., Ed.; American Chemical Society: Washington, DC, 1965.
- Simic, M.; Neta, P.; Hayon, E. *J. Phys. Chem.* **1969**, *73*, 3794.
- Frost, A. A.; Pearson, R. G. *Kinetics and Mechanism*; John Wiley & Sons, New York, 1953; Chapter 3, pp 28–31.
- Hugh, G. L. *Optical Spectra of Nonmetallic Inorganic Transient Species in Aqueous Solution*; Nat. Stand. Ref. Data, Nat. Bur. Stand. (U.S.) 69; U.S. Government Printing Office: Washington D.C., 1981. and references therein.
- Wherland, S. *Coord. Chem. Rev.* **1993**, *123*, 169.
- Kumar, K.; Rotzinger, F. P.; Endicott, J. E. *J. Am. Chem. Soc.* **1983**, *105*, 7064.
- Ronco, S.; VanVlierberge, B.; Ferraudi, G. *Inorg. Chem.* **1988**, *27*, 3453.
- Tait, A.; Hoffman, M. Z.; Hayon, E. *Inorg. Chem.* **1976**, *15*, 934.
- Marcus, R. A.; Sutin, N. *Biochim. Biophys. Acta* **1985**, *811*, 265.
- Brown, G. M.; Sutin, N. *J. Am. Chem. Soc.* **1979**, *101*, 883.
- (a) Margenau, H.; Murphy, G. M. *The Mathematics of Physics and Chemistry*, 2nd ed.; Van Nostrand: New York, 1966. (b) Wilkins, R. G. *Kinetics and Mechanism of Reactions of Transition Metal Complexes*, 2nd ed.; VCH: New York, 1991; Chapter 5, pp 262–269.
- Szalda, D. J.; Macartney, D. H.; Sutin, N. *Inorg. Chem.* **1984**, *23*, 3473.
- Hupp, T. J.; Weaver, M. J. *Inorg. Chem.* **1983**, *22*, 2557.
- (a) Ferraudi, G. *Elements of Inorganic Photochemistry*; John Wiley & Sons: New York, 1988; Chapter 1, pp 21–28 and (b) Chapter 5, pp 122–134, 225–228 (see also references therein). (b) Ferraudi, G. *Elements of Inorganic Photochemistry*; John Wiley & Sons: New York, 1988; Chapter 5, pp 122–134, 225–228 (see also references therein).
- Lever, A. B. P. *Inorganic Electronic Spectroscopy*, 2nd ed.; Elsevier: New York, 1984.
- Gaspar, A. B.; Seredyuk, M.; Gutlich, R. *Coord. Chem. Rev.* **2009**, *48*, 6130.
- Spiering, H.; Kohlhaas, T.; Romstedt, N.; Hauser, A.; Bruns-Xilmaz, C.; Kusz, J.; Gutlich, P. *Coord. Chem. Rev.* **1999**, *192*, 629.
- Decurtins, S.; Gutlich, P.; Hasselbach, K. M.; Hauser, A.; Spiering, H. *Inorg. Chem.* **1985**, *24*, 2174.
- Gutlich, P. In Spin crossover in iron(II) complexes. *Struct. Bonding (Berlin)* **1981**, *44*, 83.

JP911644E